AIAA Guidance, Navigation, and Control Conference and Exhibit
5-8 August 2002, Monterey, California

AIAA 2002-4925

Pursuit Display Review and Extension to a Civil Tilt Rotor Flight Director

Gordon H. Hardy*

Northrop Grumman Information Technology
NASA Ames Research Center, Moffett Field, CA

Abstract

This paper reviews almost thirty years of developing pursuit displays at the NASA Ames Research Center and shows how this work was applied to a Civil Tiltrotor. It then uses this previous work to develop an "Inverse" flight director to reduce pilot workload during the transition from the frontside to backside configuration while still preserving the advantages of the basic pursuit displays. The results from the Vertical Motion Simulator at NASA Ames showed that satisfactory performance and handling qualities were obtained for the transition from the cruise frontside to the final approach and landing backside configuration for a precision descending, decelerating, and turning approach under instrument conditions with normally expected crosswinds and turbulence.

Introduction

A conceptual drawing of a Civil Tiltrotor transport used for NASA studies, CTR-4/95, is shown in Figure 1. It uses rotor tilt to achieve efficient cruise flight while maintaining vertical landing capability. Piloted flight control of this vehicle is a challenging task, particularly for the transition from the cruise "frontside" (or CTOL) to the final approach and landing "backside" (or helicopter) configuration. This is especially true for a precision descending, decelerating, turning, and time constrained approach. Previous simulations, Decker, et al,[1-3] of tilt rotor aircraft at the NASA Ames Research Center have all had various levels of difficulty with this task due to both display and control system deficiencies. This paper will concentrate on the display issues. The most recent of these simulations have used the pursuit displays successfully used in previous NASA Ames V/STOL flight and simulation programs by Hynes, et al,[4] Merrick, et al, [5-7] and Franklin, et al. [8] These previous simulation programs had demonstrated the advantage of pursuit displays in combining situational awareness with command information. This paper first reports on the application of this previous work to the CTR-10 simulation conducted on the NASA Ames Vertical Motion Simulator, VMS, during the summer of 2001. Next, the pursuit displays are used to develop an "Inverse" flight director that allows the pilot to make the transition from the CTOL airplane to the landing helicopter configuration with reduced workload. While these displays were also used for the take-off, go-around, and climb-out tasks, this paper will concentrate on the precision approach task. Detailed results of the CTR-10 simulation are reported in a separate paper by Decker, et al. [9] being presented concurrently in the AIAA Modeling and Simulation Technologies Conference.

Pursuit Displays

The pursuit displays developed in the references noted above significantly reduced the workload of the pilot while still preserving good situational awareness. Hynes, et al [4] is a good summary of previous work on this type of display up through the NASA Quiet STOL Research Aircraft, QSRA, program and includes the work of Bray, et al. [10] which led to the present CTOL HUD formats. The present paper includes further refinements mainly from the work conducted during the VSTOL Systems Research Aircraft, VSRA, program reported on in References 5-8. The displays from the VSRA program were also adapted to the joint industry/NASA High Speed Research, HSR, program for the proposed High Speed Civil Transport, HSCT, and the for the Joint Strike Fighter program, JSF. An adaptation of the displays of the present report were used for the USAF/Boeing Advanced Theater Transport in Super-STOL flight during a recent simulation at the NASA Ames Research Center.

Figure 1. Civil Tilt Rotor

* Senior engineer.

Reference 4 states that prerequisite to display development, "aircraft handling under visual conditions should be satisfactory to the pilot, either naturally or with the aid of control augmentation." The pursuit displays described here have in general been used with good handling aircraft. A wide variety of control response types has been used, ranging from basic aircraft to flight path rate command systems.

Display Description

Figure 2 shows the unique elements of these displays. The flight path symbol (circle with a tail view of wings and tail) is shown near the center of the display and is similar to that used for several operational HUDs (e.g. Desmond, et al.[11]). For the CTR-10 simulation, no HUD was used and this display format was presented on the head down Primary Flight Display, PFD. The flight path symbol represents the velocity vector and is driven laterally by track angle over the ground, ψ, and vertically by the climb angle (arctan (climb rate/ground speed)), γ. The subscript Q is shown on γ in Figure 2 to indicate that quickening has been added to the basic climb angle to improve pilot control. The quickening is discussed later.

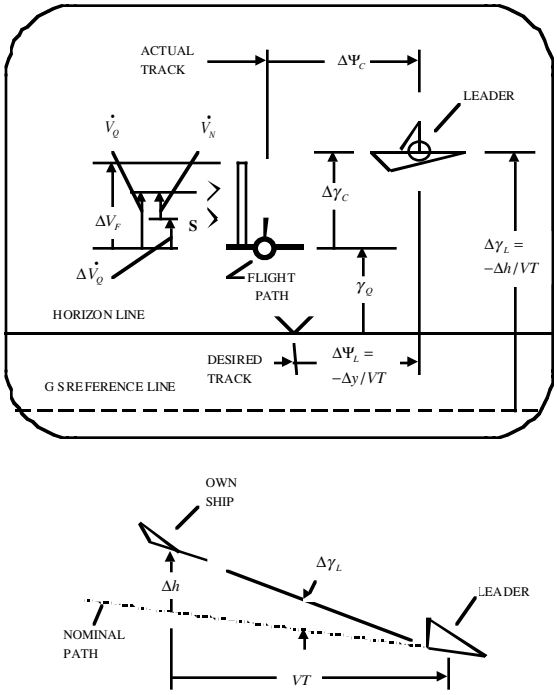

Figure 2. Pursuit Display Elements

The vertical tape on the left wing of the flight path symbol shows the error in true airspeed, ΔV_F, from the commanded value from the Flight Management System, FMS, for the precision approach. The subscript F is used to show that it is filtered to prevent excessive turbulence from making the display noisy. If the vehicle is faster than the commanded value, the tape moves above the wing.

There are two carets off the left wing of the flight path symbol, an open one and a scheduled, "s", or nominal one. The open caret, $\dot{V}_Q$, indicates the total rate of change of filtered and quickened true airspeed with respect to the left wing of the flight path symbol. Again, the quickening is discussed later. If airspeed is increasing, the caret moves above the wing. If the caret is scaled in g's on the display, it has the important property of indicating the so-called potential flight path angle. This is shown by the equation of motion along the velocity vector for small angles:

$$\frac{\dot{V}}{g} + \gamma = \frac{F_X}{W}$$

If the sum of the external forces along the flight path, F_X, is held constant (i.e. configuration, speed, power, and angle of attack all held constant), then acceleration along the flight path can be traded for an increase in flight path angle. A potential flight path angle can then be defined as the maximum flight path that can be maintained with zero acceleration along the flight path at the present configuration and speed. This is particularly useful during wind shears or during the climb phase.[12–13] The "s" caret, $\Delta\dot{V}_Q$, indicates the deviation from the nominal rate of change of true airspeed for an approach with a nominal or "scheduled" acceleration (or deceleration). $\dot{V}_N$ is the nominal or "scheduled" rate of change of true airspeed for the approach. $\dot{V}_Q$ is then the sum of $\Delta\dot{V}_Q$ and $\dot{V}_N$. $\Delta\dot{V}_Q$ and $\dot{V}_N$ are discussed in more detail later.

During approach, the pilot uses the airspeed error tape and the appropriate airspeed rate caret to control to the commanded airspeed from the FMS. He does this by using the controls appropriate for the aircraft configuration to place the caret opposite the tape. If the aircraft is fast this decelerates it. The tape is scaled such that if the caret is controlled opposite the tape with the same display magnitude as the tape this will cause the aircraft's actual airspeed to exponentially converge on the commanded airspeed with an appropriate time constant. If the pilot controls $\dot{V}_Q$ such that:

$$\dot{V}_Q = -\frac{\Delta V_F}{K}$$

where $\dot{V}_Q$ and $\frac{\Delta V_F}{K}$ are in display units of degrees and K is the velocity error scaling (knots/degree), then for velocity in units of fps:

$$\frac{\dot{v}}{g}(57.3) = -\frac{\Delta v/1.69}{K}$$

or:

$$\frac{57.3(1.69)K}{g}\left(\dot{v}\right) + \Delta v = 0 \qquad \tau = \frac{57.3(1.69)K}{g}$$

For recent work, K has been chosen as ≈3.3 knots of airspeed error/display degree to give a time constant, τ, of about ten seconds. This simple analysis is only approximate since filtered airspeed error and quickened airspeed rate are displayed instead of the actual values but the result is approximately correct in practice.

The leader aircraft symbol is the perspective delta wing vehicle with the pusher propeller (from Reference 5) at the upper right of Figure 2. It represents a true perspective of a leader aircraft flying a perfect trajectory T seconds ahead. The leader perspective reinforces deviation from the desired path not available in earlier formats. It is driven vertically as shown at the bottom of Figure 2. For small angles, the leader is $-\Delta h/VT$ (V is groundspeed) above the nominal glide path shown by the "GS Reference Line" on the display. Similarly, the leader is $-\Delta y/VT$ to the right of the nominal track where Δy is the lateral distance perpendicular to the nominal flight path (positive to the right). For lateral and vertical flight path control, the pilots task is to control the flight path symbol onto the leader symbol using the controls appropriate for the aircraft configuration. To a first order, this will cause the aircraft's actual trajectory to exponentially converge on the desired with a time constant of T seconds. For Δh, for example, if the pilot controls the flight path (referenced to the nominal path) to the leader, then for small angles:

$$\Delta\gamma = \frac{\Delta\dot{h}}{V} = -\frac{\Delta h}{VT}$$

and:

$$T\Delta\dot{h} + \Delta h = 0$$

Values of T have typically varied from 5 to 15 seconds. The larger values are used where less precision is required and it is desired to maintain a low workload. For CTR-10 on the approach, T was 15 seconds above 1500 feet and varied linearly with altitude from 15 seconds to 5 seconds at 100 feet. It was a constant 5 seconds below 100 feet. While in the past different values of T have sometimes been used for lateral and flight path control, for CTR-10 the same values were used for both tasks. As in controlling airspeed, this simple analysis is only approximate since quickened flight path is displayed instead of the actual value.

Details of the pilot tasks are discussed in more detail in the next three sections.

Lateral Path Control

As mentioned above, the pilot's lateral task is to control the flight path symbol onto the leader symbol. He uses bank angle control for this task. The pilot must realize that the leader is track command and that he is turning the aircraft to the desired track. It is not bank angle command as in a conventional flight director. If he uses it as a bank angle command, there is a tendency to over-control in track. After a short amount of experience, this tendency usually disappears and precise lateral control is achieved with no additional conditioning on the symbols.

Vertical Flight Path Control

Flight path and airspeed control are much more difficult tasks. This is especially true for a precision descending, decelerating, turning, time constrained approach with a transition from airplane to helicopter configuration. The upper part of Figure 3(a) shows a simplified block diagram of the flight path control task. The desired change in flight path, $\Delta\gamma_C$, is from Figure 2 and is the amount required to place the flight path symbol on the leader. The pilot's inceptor is represented by the general notation, $\boldsymbol{I}$, as it changes depending on the aircraft configuration, pitch for flight path in the aircraft configuration and throttle/collective in the helicopter configuration. The aircraft dynamics are represented by the first order system with a steady state value of γ_I (to a unit inceptor input) and a heave time constant of τ_H seconds. This simple model is representative of many pitch attitude stabilized vehicles for the time frame of interest (≈1-4 seconds) to the pilot for a multi-axis task. If the vehicle has a significantly slow heave response, τ_H > ≈1.0 seconds, then the pilot has a tendency to over-control in flight path and has to provide additional compensation which increases his workload. As shown later, the tilt rotor has dynamics that often fall in this category.

The bottom of Figure 3(a) shows the same system but with quickening added to the pilots display of flight path to help alleviate this problem. For this simple case, the quickening is a simple first order washout of the inceptor, pitch or throttle. If the gains in the quickening are chosen correctly to match the aircraft in the pilots control time frame, the aircraft plus quickening becomes a simple gain, the aircraft's steady state response in flight path, γ_I. This allows the pilot to close a much tighter loop on the quickened flight path, $\Delta\gamma_Q$, than possible on the actual flight path, $\Delta\gamma$. With reasonable pilot gains, the effective closed loop time constant for this task can be very short. On the order of a few tenths of a second for the throttle and somewhat longer for pitch. This reduces the

pilot workload significantly and makes for an efficient multi-axis task strategy.

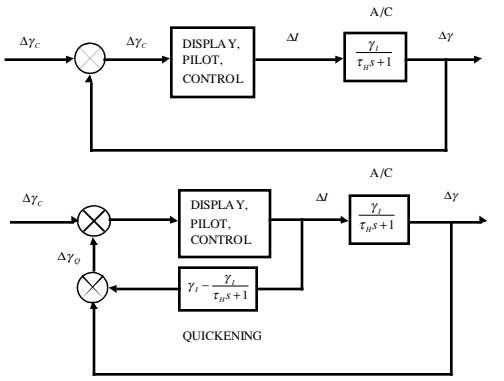

(a) Concept

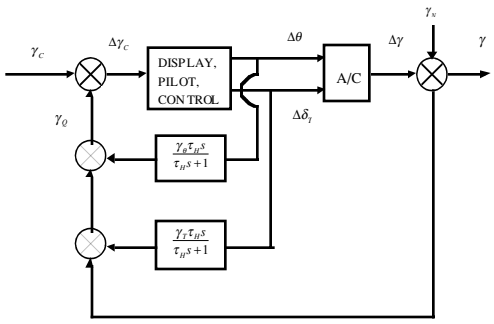

(b) Final Design

Figure 3. Flight Path Control

In the general case, especially during transition, both pitch and throttle are used to control flight path. This is shown in Figure 3(b) for the system as implemented for CTR-10. The quickening is shown as first order washouts. As shown in the work of Merrick,[6] if the nominal values of pitch and throttle are changing, the changes in the inceptors from nominal must be used for the quickening to provide accurate control. This requires that the nominal values of pitch and throttle be generated by the FMS. The steady state response gains of the aircraft from trim to pitch, γ_θ, and throttle, γ_T, vary with aircraft configuration, velocity, and flight path angle. The heave time constant is also a function of these same variables. For CTR-10, since the flaps were scheduled with velocity and nacelle angle, these gains for the washout filters were stored in the display system as a function of equivalent velocity, flight path angle, and nacelle angle. These response gains and heave time constant were determined by a combination of inceptor step inputs into a linear system based on stability derivatives and on nonlinear simulation step responses to the inceptors. Figure 4 shows an example of the nonlinear simulation. The first plot is the aircraft's pitch response to an aft cyclic pulse.

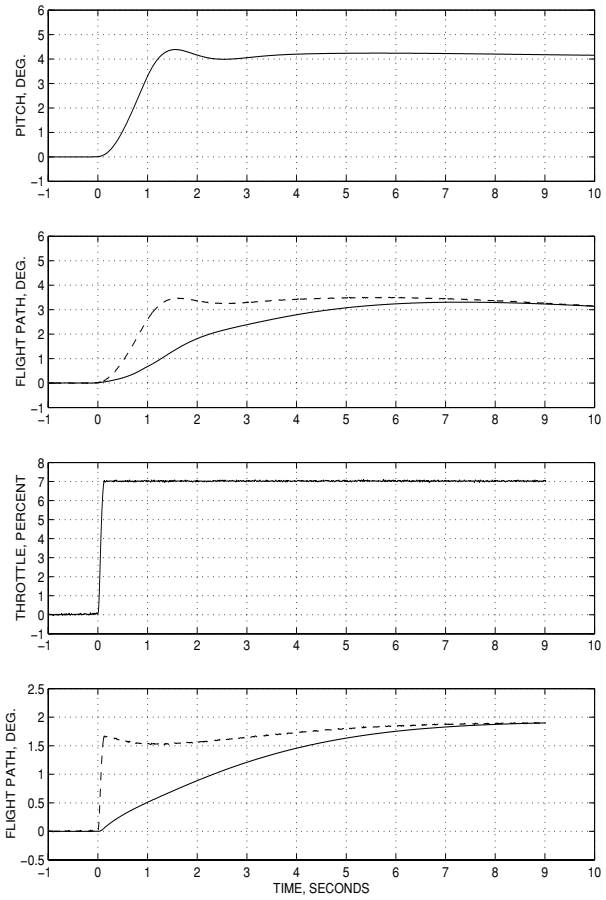

Airspeed=110 Knots, Flight Path=0 degree, Nacelle=60 degrees

Figure 4. Simulation Flight Path Responses to Pitch and Throttle Inputs

The second plot shows the actual and quickened flight path responses. The third and fourth show the results for a throttle step. For this flight condition γ_θ was approximated from Figure 4 as 0.69 degrees/degree and γ_T as 0.26 degrees/percent throttle. The heave time constant was 2.1 seconds. These approximations are valid for the pilot control time frame of 1-4 seconds.

Nacelle angle changes were considered as configuration changes and no additional display compensation was needed. The nacelle rates were tailored to give minimum flight path change for pitch and throttle settings appropriate to the approach.

Airspeed Rate Control

Figure 5(a) shows the simplified and quickened block diagram for the airspeed rate control task. For commanded airspeed rate, $\Delta\dot{V}_C$, the pilot uses the control strategy discussed earlier. This figure is similar in format to the lower part of Figure 3(a) for the flight path task. Because the time constants of the aircraft's response in speed are very slow compared to the pilots control time frame, the aircraft's airspeed response to the general inceptor, I, can

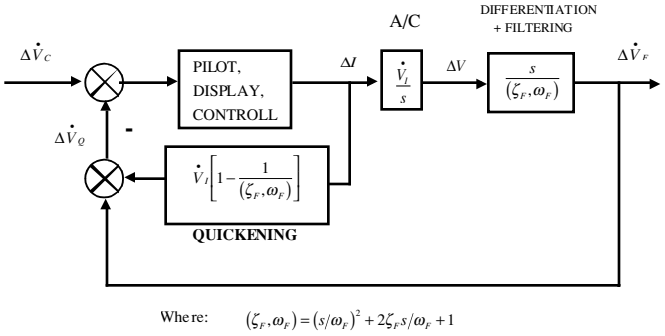

(a) Concept

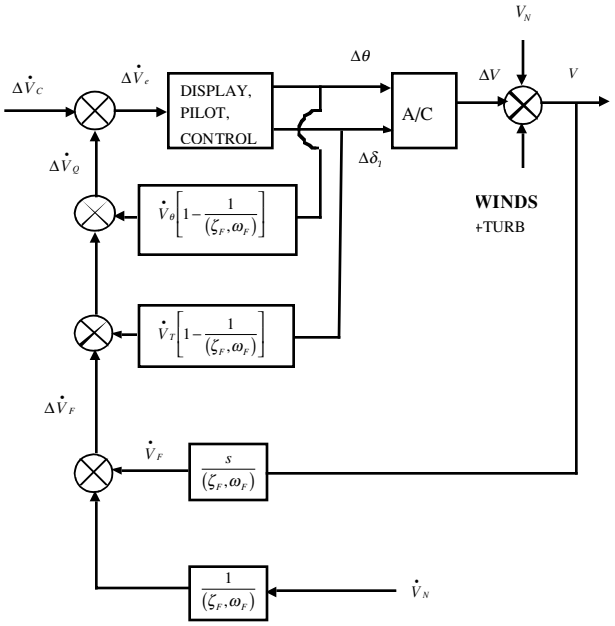

(b) Used for CTR-10

Figure 5. Airspeed Rate Control

be represented by an integrator and a gain, $\dot{V}_I$. To obtain airspeed rate for the pilot's display, the measured airspeed is differentiated and then filtered to remove the high frequency noise due to atmospheric turbulence. A second order filter is used because of the differentiation. The differentiation and filtering are combined into a washout filter for implementation. The differentiation cancels out the airframe integrator and the quickening becomes a second order washout filter as shown in Figure 5(a). As in the flight path control task, with quickening the aircraft plus quickening becomes a simple gain, the aircraft's steady state response in airspeed rate, $\dot{V}_I$. Again, the effective closed loop time constant for control of quickened airspeed rate, $\Delta\dot{V}_Q$, can be very short, reducing the pilot's workload significantly.

As in the case for flight path control, both pitch and throttle are used to control airspeed rate. This is shown in Figure 5(b) for the system as implemented for CTR-10. The deceleration rate of the nominal trajectory, $\dot{V}_N$, is obtained from the FMS, filtered and subtracted from $\dot{V}_F$ to obtain $\Delta\dot{V}_F$. Adding the quickening gives $\Delta\dot{V}_Q$ which drives the "s" caret in Figure 2. This is the caret used for a decelerating approach. For $\dot{V}_N \equiv 0$, the two carets are coincident. The steady state response gains of the aircraft from trim to pitch, $\dot{V}_\theta$, and throttle, $\dot{V}_T$, are also stored in the display system as a function of equivalent velocity, flight path angle, and nacelle angle. These response gains were determined by a combination of inceptor step inputs into a linear system based on stability derivatives and on nonlinear simulation step responses to the inceptors. Figure 6 shows the nonlinear simulation actual, filtered, and quickened responses for the same example as for flight path control. For reference, the actual airspeed rate is from the equations of motion. For this example the response gains were determined using the stability derivatives and checked with the nonlinear results. $\dot{V}_\theta$ was approximated as 0.79 display degrees/degree pitch and $\dot{V}_T$ as 0.23 display degrees/percent throttle. The airspeed rate second order filter damping ratio, ζ_F, was 0.8 and the natural frequency, ω_F, was held constant (0.6 rps) for this example below 100 knots ground speed and varied inversely with ground speed above 100 knots. This was done since at the higher speeds less precision was required and the frequency content of the turbulence is higher. As seen in Figure 6, for both pitch and throttle, it appears that slightly lower values of the response gains would have provided a better match of quickened to actual response in the pilots control time frame.

While the response gains for airspeed rate were not "optimal", no control problems were noted. An important feature of the displays is that high precision in the quickening is not needed.

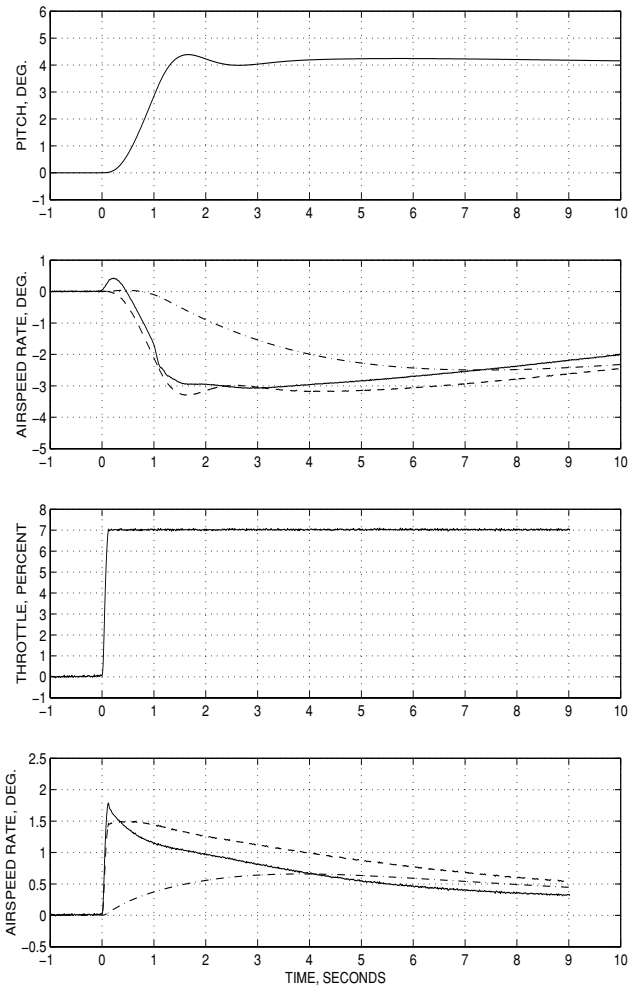

Airspeed=100 Knots, Flight path=0 degree, Nacelle=60 degrees

—— Actual –·– Filtered – – Quickened

Figure 6 Simulation Airspeed Rate Responses to Pitch and Throttle Inputs

"Inverse" Flight Director

In general, as noted in the discussion of pursuit display flight path and airspeed rate control, the pilot must use both inceptors (pitch and throttle) to control either flight path or airspeed. What combination to use varies with each aircraft configuration, speed, and flight path angle. While the pilot can learn this, it significantly increases his workload. This is especially true for a tightly constrained, precision approach. From the previous discussions of flight path and airspeed rate control, steady state flight path and airspeed rate response to pitch and throttle inputs is given, in the pilot's control time frame, by:

$$\Delta\gamma_{SS} = \Delta\gamma_Q = \gamma_\theta \Delta\theta + \gamma_T \Delta\delta_T$$

$$\Delta\dot{V}_{SS} = \Delta\dot{V}_Q = \dot{V}_\theta \Delta\theta + \dot{V}_T \Delta\delta_T$$

To show the difficulty of the pilot's task for the CTR-10 tiltrotor transition from frontside to backside, the response gains in the above equations are shown for three flight conditions (all for level flight):

Frontside (nacelles=0, V=250):

$$\begin{pmatrix} \gamma_\theta & \gamma_T \\ \dot{V}_\theta & \dot{V}_T \end{pmatrix} = \begin{pmatrix} 1.0 & 0 \\ 0.98 & 0.21 \end{pmatrix}$$

Transition (nacelles=60, V=110):

$$\begin{pmatrix} \gamma_\theta & \gamma_T \\ \dot{V}_\theta & \dot{V}_T \end{pmatrix} = \begin{pmatrix} 0.69 & 0.26 \\ 0.79 & 0.23 \end{pmatrix}$$

Backside Approach (nacelles=80, V=50):

$$\begin{pmatrix} \gamma_\theta & \gamma_T \\ \dot{V}_\theta & \dot{V}_T \end{pmatrix} = \begin{pmatrix} 0.34 & 0.26 \\ 1.0 & 0.02 \end{pmatrix}$$

It can be seen that the throttle has no practical effect on flight path (γ_T) frontside and almost no effect on speed change ($\dot{V}_T$) backside. For the transition case, the throttle effects both flight path and speed change. The flight path response to pitch (γ_θ) gradually decreases as the vehicle transitions from frontside to backside.

From the equations above for $\Delta\gamma_Q$ and $\Delta\dot{V}_Q$, the required changes in pitch and throttle to control the quickened values of flight path and airspeed rate to the commanded values of Figures 3(b), γ_C, and 5(b), $\Delta\dot{V}_C$, then will be:

$$\begin{pmatrix} \theta_C \\ \delta_{TC} \end{pmatrix} = \begin{pmatrix} \theta_\gamma & \theta_{\dot{V}} \\ \delta_\gamma & \delta_{\dot{V}} \end{pmatrix} \begin{pmatrix} \Delta\gamma_C \\ \Delta\dot{V}_e \end{pmatrix}$$

where:

$$\begin{pmatrix} \theta_\gamma & \theta_{\dot{V}} \\ \delta_\gamma & \delta_{\dot{V}} \end{pmatrix} = \begin{pmatrix} \gamma_\theta & \gamma_T \\ \dot{V}_\theta & \dot{V}_T \end{pmatrix}^{-1}$$

These are the "Inverse" flight director commands. Figure7 summarizes this and shows how the airspeed rate command, $\Delta\dot{V}_C$, is calculated. V_C comes from the FMS and the gain $1/K_S$ sets the airspeed convergence rate. The first order filter with the time constant of τ_T filters out the high frequency turbulence in the measured airspeed error. τ_T was held constant (≈ 1.5 - 2.5 seconds) below 100 knots ground speed and varied inversely with ground speed above 100 knots.

Figure 8 shows the PFD used for CTR-10 with the flight director commands included. The pitch command is the solid caret on the right wing of the flight path symbol and in the figure is commanding a small pitch up. The throttle command is the "handle" notched into the left wing and in the figure is commanding a small reduction in thrust

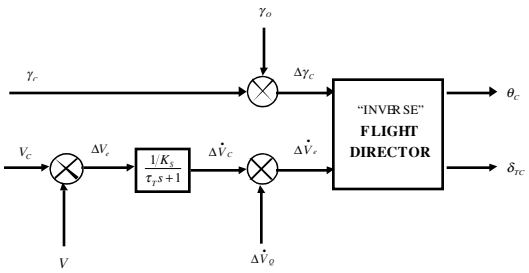

Figure 7. "Inverse" Flight Director

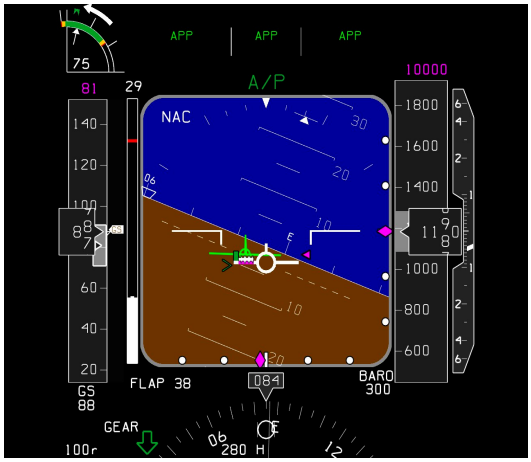

Figure 8. PFD on Base Turn showing the pitch and TCL flight directors

(push the handle down into the wing). The remaining flight path elements are described in Figure 2. The airspeed error in Figure 8 is about 7 knots fast and the raw glide path deviation is near zero. The flight director commands are consistent with this condition. For this flight condition with a 75 degree nacelle angle, it takes the right combination of pitch and throttle to correct an airspeed error without affecting the flight path.

Also for the small "right of course" raw lateral deviation shown in Figure 8, the leader is showing a small left track change ($\approx 5^{\circ}$) is required.

The location of the flight director commands is consistent with the flight path centered display philosophy. All the required situation and command information is located with the flight path symbol and reduces the pilots scan requirements.

Approach Profile

Figure 9 shows the Navigation Display for the descending, decelerating, and turning approach used for CTR-10. Initial bank angles in the base turn varied from 15 – 25 degrees. The nominal glide slope reference was –3.0 degrees on downwind and through the base turn, capturing a –9.0 degree path for the final straight in approach at about 800 feet above runway 28 at the SFO Vertiport. Figures 10(a) and (b) show the nominal, or scheduled, trajectory values stored in the FMS used by the display system. The nacelles were commanded by the pilot in discrete increments. He commanded the nacelle transition from 0 – 60 degrees at about 195 KEAS. Speed stabilized at 110 knots for a few seconds before the nacelles were commanded discretely to 75 degrees. Speed then stabilized at 80 knots for a few seconds before the nacelles were commanded to the final approach

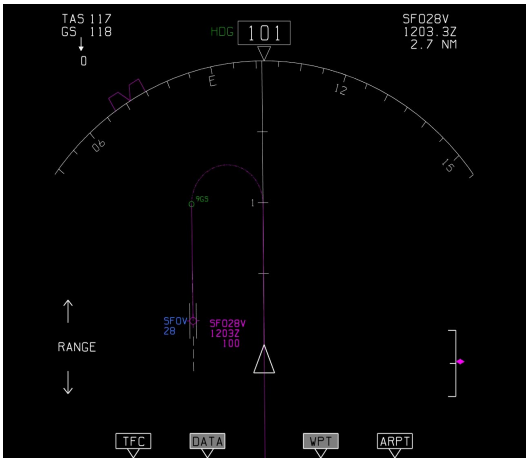

Figure 9. Navigation Display showing the tight downwind SFO verti-port approach

setting of 80. At the landing decision point (200 feet) the nacelles were commanded to the final landing setting of 86 degrees. From the first plot in Figure 10(b), it can be seen that the deceleration level is about one knot/second. The approaches were flown IFR down to 200 feet with the landing task performed visually. The second and third plots of Figure 10(b) show that the nominal values of the pilots inceptors, thrust control lever and pitch, varied slowly. In fact, the nominal throttle was essentially constant, only increasing for the constant speed final nine degree glide slope. This contributed to a low pilot workload.

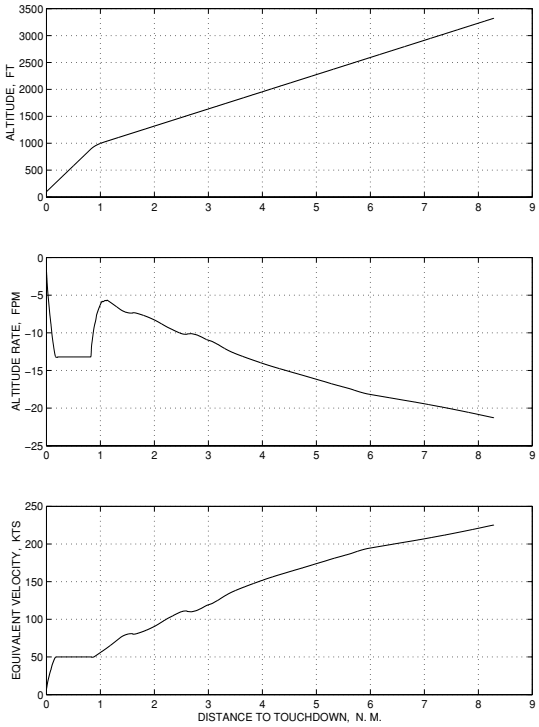

Figure 10(a) Scheduled trajectory values from the Flight Management System

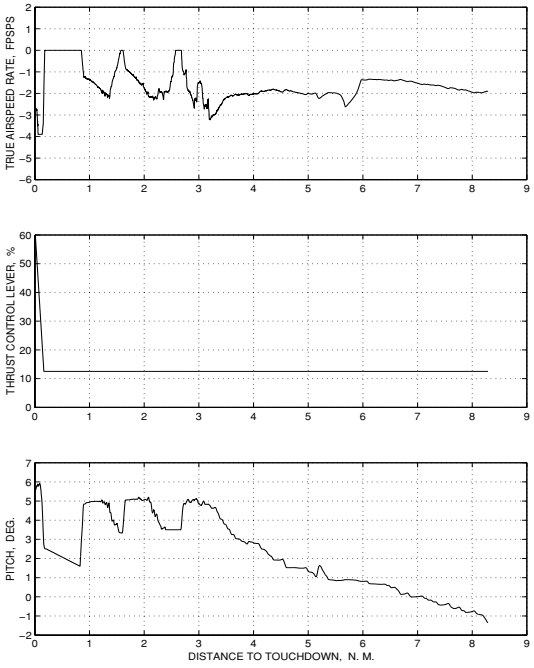

Figure 10(b) Scheduled trajectory values from the Flight Management System

Results

All the results shown in reference 9 for the main CTR-10 experiment used a single set of gains for the flight director. During the conduct of this experiment it was realized that the gains used in the display airspeed/airspeed rate filtering were allowing the flight director to be quite active in the presence of turbulence. This was particularly troublesome during and after nacelle conversion when pitch was the primary controller for airspeed errors. This resulted in a high workload during this phase of the approach.

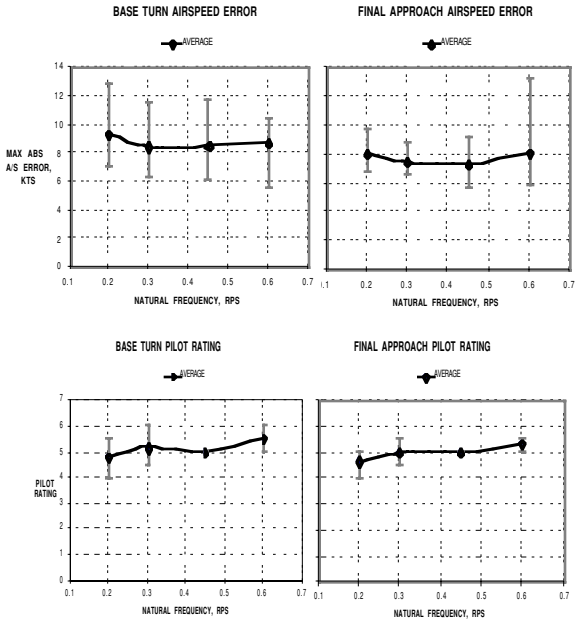

Figure 11 Airspeed rate filter natural frequency variation, $1/K_S = 0.3$, $\tau_T = 1.5$

In order to examine the effect of this issue, a short fixed base experiment was conducted using three pilots in the CTR-10 cab. Two filtering gains were varied, the time constant on the airspeed error filter (τ_T in Figure 7) and the natural frequency in the airspeed error rate filter (ω_F in Figure 5(b)). The gain $1/K_S$ in Figure 7 on the airspeed error was also varied. Figure 11 shows the effect of varying the airspeed rate filter natural frequency, ω_F for the most difficult flight card used for CTR-10. The left column shows the airspeed error and pilot's ratings [14] for the base turn, and the right column shows the ratings for the straight-in final approach. The average pilot rating is shown along with the maximum and minimum values. There is a slight improvement in pilot rating with a decrease in the natural frequency (and decrease in the flight director activity) while the airspeed performance did not

degrade down to about 0.3 rps. Below 0.3 rps, airspeed control degraded somewhat. Variations in the other two

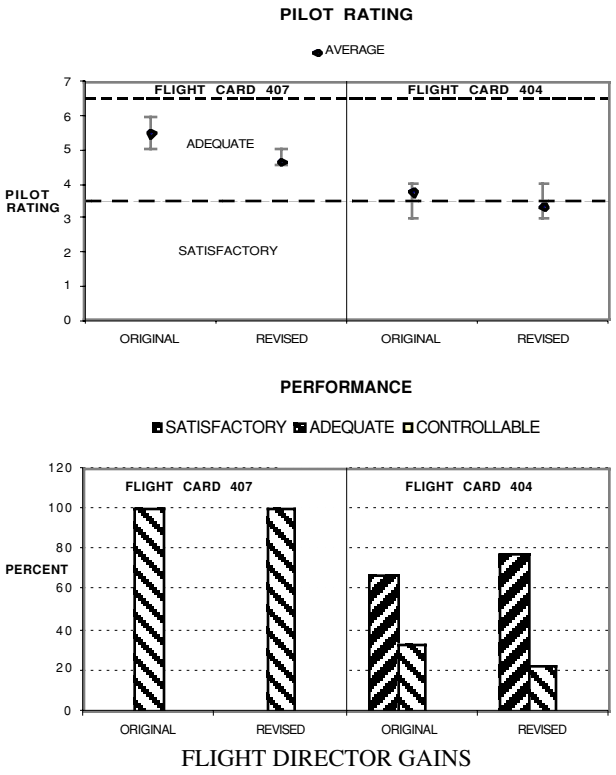

FLIGHT DIRECTOR GAINS

Flight Card 407: 25 deg bank turn, 20 Kt crosswind, 4.5 fps RMS turbulence
Flight Card 404: 20 deg bank turn, 10 Kt crosswind, 2.5 fps RMS turbulence

Figure 12 Effect of Flight Director gains on base turn pilot rating and performance

gains did not have as significant an effect on the performance and pilot rating.

Figure 12 shows the effect of the revised set of gains chosen versus the original set on the base turn pilot ratings and performance as this was the highest workload segment of the approach. The results are shown for flight card 407 (base turn with an initial 25 degree nominal bank, 20 knot tail wind on the base turn, and turbulence with RMS=4.5 fps) and flight card 404 for a more normal situation (base turn with an initial 20 degree nominal bank, 10 knot tail wind on the base turn, and turbulence with RMS=2.5 fps). The pilot rating for flight card 407 improved almost one rating unit while for the more normal flight situation of flight card 404 the average pilot rating improved to marginally satisfactory. More dramatic was the improvement in pilot comment. A typical pilot comment for flight card 407 for the original flight director gains was, "control activity high, extensive compensation" while with the revised gains was, "reasonable workload, less nervous than previous (original gains)". A typical pilot comment for card flight 404 for the original flight director gains was, "lots of pitch flight director activity, fairly high workload" while with the revised gain was, "display a little active".

The performance summary in Figure 12 summarizes the three performance metrics for this flight segment; maximum glide slope error, maximum lateral error, and maximum airspeed error. Each evaluation run is categorized by the worst performance for each of the three metrics. For example, to be categorized as satisfactory, all three metrics must be in the satisfactory range. If only one metric drops to adequate, the category becomes adequate for that run. Each performance category is then presented as a percentage of the total number of runs. Maximum satisfactory and adequate values for glide slope and lateral errors were 1/2 and one dot respectively. For this segment of the approach, one dot of localizer equaled 300 feet and one dot of glide-slope equaled 100 feet. For max airspeed error satisfactory and adequate performance corresponded to 5 and 10 knots respectively. The results are dominated by the airspeed error and for flight card 407 were all adequate. For the more normal flight situation of flight card 404, 78% of the performance results with the revised gains were satisfactory. With 25 degrees of nominal bank and a 20 knot tailwind on the base turn, flight card 407 was too aggressive for good ratings.

Conclusions

- The displays provided a good combination of situational and command information with all information flight path centered. This required a minimal scan to completely access the flight situation. The leader aircraft provided scaled raw glide path and lateral deviations while the flight path symbol provided conditioned information on the actual state. The airspeed error tape and the airspeed rate carets provided a complete assessment of the airspeed situation. The airspeed rate caret had the additional significance of showing the potential flight path angle which is particularly useful for wind shear and marginal power climb situations.
- By basing the "Inverse" flight director commands on the quickened flight path and acceleration caret, the flight director task can have very short effective time constants and consequent low pilot workloads for a precise multi-axis task.
- The displays were easy to implement. The adaptation of the pursuit displays from previous work was straight forward. With reasonable conditioning (quickening) on the flight path and airspeed rate, the "Inverse" flight director implementation was also straight forward. Little tuning of the display elements was required.
- While the work reported on in this paper concentrated on the precision approach, the display concepts were

easily extended to other flight phases such as take-off, go-around, and climb.

- The precision descending, decelerating, and turning approach profile with a nominal initial 25 degree bank angle base leg turn, 20 knots of tailwind on the turn, and moderate turbulence was aggressive and would not be recommended.
- The approach profile with a nominal initial 20 degree bank base leg turn, 10 knots of tailwind on the turn, and light turbulence was less aggressive and with the controls and displays developed provided borderline satisfactory pilot ratings and performance results.

References

[1] Decker, W.A., "Piloted Simulator Investigations of a Civil Tilt-Rotor Aircraft On Steep Instrument Approaches," American Helicopter Society 48th Annual Forum, June 1992.

[2] Decker, W.A., Bray, R.S., Simmons, R.C., and Tucker, G.E., "Evaluation of Two Cockpit Display Concepts for Civil Tiltrotor Instrument Operations on Steep Approaches," American Helicopter Society Piloting Vertical Flight Aircraft: A Conference on Flying Qualities and Human Factors, San Francisco, CA, January 1993.

[3] Decker, W.A., "Handling Qualities Evaluation Of XV-15 Noise Abatement Landing Approaches Using A Flight Simulator," American Helicopter Society 57th Annual Forum, May 2001.

[4] Hynes, C. S., Franklin, J.A., Hardy, G. H., Martin, J. L., and Innis, R. C., "Flight Evaluation of Pursuit Displays for Precision Approach of Powered –Lift Aircraft," *AIAA Journal of Guidance and Control,* July-August 1989, pp. 521-529.

[5] Merrick, V. K., Farris, G. G., and Vanags, A. A., "A Head Up Display for Application to V/STOL Aircraft and Landing," NASA TM 102216, January 1990.

[6] Merrick, V. A., "Some VTOL Head-Up Display Drive-Law Problems and Solutions," NASA TM 104027, November 1993.

[7] Merrick, V. A. and Jeske, J. A., "Flightpath Synthesis and HUD Scaling for V/STOL Terminal Area Operations," NASA TM 110348, April 1995.

[8] Franklin, J. A., Stortz, M. W., Borchers, P. F., and Moralez III, E., "Flight Evalutions of Advanced Controls and Displays for Transition and Landing on the NASA V/STOL Systems Research Aircraft," NASA TP 3607, April 1996.

[9] Decker, W.A. and Hardy, G.H., "Civil Tiltrotor Transport Procedure and Requirement Development Using a Flight Simulator," AIAA Paper 2002-4530, August 2002.

[10] Bray, R.S. and Scott, B.C., "A Head-Up Display Format for Transport Aircraft Approach and Landing," NASA CP-2170, 1980.

[11] Desmond, J. P. and Ford, D. W., "Certification of a Holographic Head-Up Display for Low Visibility Landings," AIAA 84-2689-CP, December 1984.

[12] Joppa, R. G. and Nicholson, R. K., "Flight Deck Displays for Managing Wind Shear Encounters," SAE 1984 Aerospace Congress and Exposition, Long Beach, CA, October 1984.

[13] Funabiki, K., Bando, T., Tanaka, K., Hynes, C. S., and Hardy, G. H., "A Method of Wind Shear Detection for Powered-Lift STOL Aircraft," AIAA Paper 93-3667, August 1993.

[14] Cooper, G.E. and Harper, R.P., "The Use of Pilot Ratings in the Evaluation of Aircraft Handling Qualities," NASA TN D-5153, April 1969.